

# Conceptual design for a dispersive XAFS beamline in the compact storage ring MIRRORCLE

Canestrari N. <sup>a,b</sup>, Roger V. <sup>b</sup>, Jeantet P. <sup>b</sup>, Leynaud O. <sup>b</sup>, Ortega L. <sup>b</sup>, Yamada H. <sup>c,d</sup>,  
Hanashima T. <sup>d</sup>, Lorenzo J.E. <sup>b</sup>, Sanchez del Rio M. <sup>a</sup>

<sup>a</sup> European Synchrotron Radiation Facility, 6, rue Jules Horowitz, 38000 Grenoble, France

<sup>b</sup> Institut Néel, CNRS-UJF, 38042 Grenoble, France

<sup>c</sup> Ritsumeikan University, 1-1-1 Nojihigashi, Kusatsu-shi, Shiga 525-8577, Japan

<sup>d</sup> Photon Production Laboratory, 1-1-1 Nojihigashi, Kusatsu-shi, Shiga 525-8577, Japan

## ABSTRACT

We present the conceptual design of a dispersive X-ray Absorption Fine Structure (XAFS) beamline for MIRRORCLE, a new compact laboratory X-ray source. This machine accelerates electrons up to 1,4,6 or 20 MeV (depending upon the model) in a ring and produces X-rays when the electrons collide onto a thin target. The radiation emitted has a white spectrum due to both synchrotron and bremsstrahlung emission. A substantial part of the electrons are recovered after collisions, and the emitted light has high flux, wide energy spectrum and a large angular dispersion.

We have opted for a simple beamline design using a collimator, slits, a curved crystal, the sample environment and a CCD. The beamline parameters (position of the mirror, ray of curvature, slit aperture, reflecting angle, *etc.*) have been optimized by defining and improving a figure of merit. This optimization allows for room constraints (distances among elements), mechanical constraints (minimum curvature radii available) and optical constraints. Further ray tracing simulations using SHADOW3 have been performed to check all the theoretical results, refine the final parameters, quantitative flux calculations and for simulating the image on the CCD camera.

**Keywords:** X-ray beamline, crystal optics, optimization, ray-tracing, XAFS.

## 1. INTRODUCTION

There is an overall interest in studying ways to bring synchrotron-like capabilities to the laboratory. These inevitably go through the availability of compact, relatively cheap and powerful X-ray sources. The MIRRORCLE sources,<sup>1</sup> developed by Prof. H. Yamada and Photon Production Laboratory (PPL), are powerful devices enabling to generate light in a wide electromagnetic spectrum (104  $\mu\text{m}$  to 0.01  $\text{\AA}$  or  $10^{-4}$  eV to 104 keV). Several kinds of interaction between electrons and matter are used to generate light in such a broad spectral range.<sup>2</sup> The purpose of this work is to study the feasibility of dispersive XAFS experiments in the range 5 - 20 keV. MIRRORCLE generates photons of these energies by coherent bremsstrahlung, from a small target, a rod of typically 10 to 250  $\mu\text{m}$  diameter. The main difference between the MIRRORCLE generator and off-the-shelf commercial lab generators is the energy at which electrons have been accelerated ( $E_e$ ) in order to produce X-rays. Where it is of the order of 60 keV to 150 keV in the latter, it ranges from 1 to 20 MeV for the former. As the electron energy is larger than  $mc^2 = 511$  keV, the emission is said to be relativistic and occurs within a cone of aperture defined by  $1/\gamma$ , where  $\gamma = E_e/mc^2$ . The lower the energy of the electrons in the ring the wider is the cone aperture with typical values of the photon divergences are  $28.5^\circ$  (1 MeV),  $7.3^\circ$  (4 MeV),  $1.4^\circ$  (20 MeV).

The key parameters of our study can be retrieved from the operation features: the size of the source is determined by the size of the target, photon divergences are determined by the electron energy. Other features such as stability of the beam, reproducibility of the source, *etc.* have been successfully tested by PPL. We lack

---

Further author information: (Send correspondence to C.N.)

C.N. : E-mail: niccolo.canestrari@esrf.eu, Telephone: +33 (0)4 76 88 29 52

S.R.M.: E-mail: srio@esrf.eu, Telephone: +33 (0)4 76 88 25 13

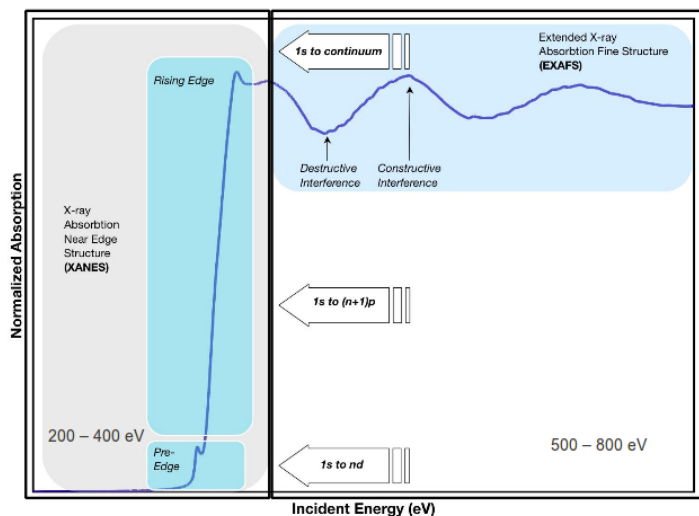


Figure 1. A typical absorption spectra (XAFS) with the different energy ranges.

of an experimental determination of the flux for this study, but theoretical values are calculated by Gambaccini et al.<sup>3</sup>

A number of techniques have been successfully developed around MIRRORCLE sources. Certainly the most well known is X-ray imaging either for medical purposes<sup>4</sup> or for non destructive inspection of materials and devices.<sup>5</sup> The high photon energies delivered by the source is an important asset in these endeavors and, as a consequence, contrast results greatly enhanced.

X-ray absorption spectroscopy (XAS) is a technique of interest in the broad community of material science. This technique allows for measuring the absorption of the sample as a function of the photon energy in the neighborhood of an atomic resonance (see Fig. 1). From this technique a number of features can be inferred such as the valence state of the absorbing atom, the local coordination as well as inter-atomic distances, etc. It has been used in a variety of applications such as speciation of ions in water, in catalysis, in the study of organometallic compounds, ion implantation, trace impurities (as in forensic examinations).

Preliminary and proof-of-principles dispersive XAFS experiments have been performed with MIRRORCLE.<sup>6</sup> The quality and beam stability of this source is mandatory and are the key for the success of these previous experiments.

A compact dispersive XAFS instrument has been studied and designed, with the aim of simultaneously measuring the full absorption spectra (within a given energy band up to 1000 eV) in a single shot, without moving any beamline component. In order to optimize the instrument we have decided to look into the energy resolution required in each part of the spectra. In the near edge features (or XANES region, X-ray absorption near edge spectroscopy, see Fig. 1) the resolution should be very good, of the order of 2 eV or better. Whereas in the extended part of the spectra (or EXAFS, Extended X-ray absorption fine structure) the required experimental resolution is about 10 eV. This type of instruments already exists at 3<sup>rd</sup> generation synchrotron light sources such as the European Synchrotron in Grenoble (beamline ID24), SOLEIL (beamline ODE), Diamond (beamline I20), or NSLS II in Brookhaven.

## 2. SIMULATION OF THE BEAMLINE

Following the criteria of simplicity, the beamline is formed by a collimator, a bent crystal of Si(111) installed on a bender, a beam stop just after the crystal to absorb the high energy photons, a sample placed in the focused beam, and a CCD camera. Such a reduced number of optical elements arises from the requirement to have a compact instrument. Before describing the different optical elements and simulations, we describe the collimator

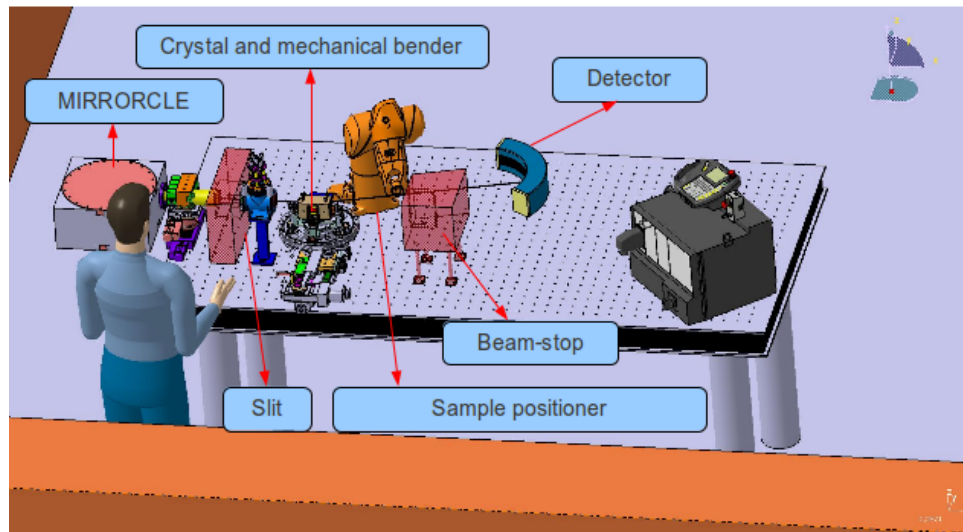


Figure 2. Virtual image of laboratory table, where MIRRORCLE source and the beamline elements are placed.

and of the beam-stop. Admittedly, one of the drawbacks of having a rather divergent beam is that unwanted photons can illuminate the different elements in the photon area and serve as secondary sources of particles (photons, electrons, neutrons,...) and hence of background. In commercial X-ray generators the collimator is the first element right after the anode. It defines the divergence of the photon beam. Often it is small as the photon energy does not exceed 50 keV and therefore photons can be stopped with a few millimeters of Pb or Ta, *etc.*

The definition of the beam path by means of a collimator is crucial in beamlines designed to work with a MIRRORCLE source. Indeed the beam contains photons of energies up to some MeV that one seeks removing (or minimizing) before they re-radiate and create background. The collimator and beamstop should be thus much larger and the design of the beamline has to do with this strong limitation imposed by their size.

As a trade-off between air absorption that limits the low energy boundary for useful experiments and the location of the absorption edges of *useful* elements, we have defined the working energy region between 5 and 20 keV. This energy interval can be expanded towards high energies if a monochromator of smaller d-spacing is chosen instead. More stringent vacuum conditions are chosen if using photons of lower energies. The optical system should deliver photons within an energy bandwidth of 500 - 1000 eV in order to cover the full EXAFS spectrum in a single exposure, and should have an energy resolution (i.e., the spread in energy for a selected point in the detector) of a few eV, to resolve the XAFS spectral features. For the sake of compactness we have decided to fix the distance source-monochromator to 1 m, and study several configurations for the distance monochromator-sample as well as different angle of scattering and types of monochromators. In the same spirit the possibility to place the sample very close to the crystal has been investigated. These parameters can be finely tuned upon specific requests.

The optimization problem is thus reduced to evaluate the possible positions of the sample, calculate focal distances, in order to fulfill the necessary energy bandwidth and resolution. It includes mechanical constraints, as well. For instance, it is not possible to bend a crystal *ab libitum*, usually a radius of curvature of 2 m is considered as a safe threshold. Moreover, the simulation takes into account that the different optical elements can not overlap. Practically the optical elements are placed on a plane, the scattering plane. The sample position can vary inside this plane, in a rectangle of 3.5 m long and 2.0 m large. The source occupies a corner of it and the crystal is placed on the long edge like in Fig. 2.

A simulation is carried out by varying the sample position on a rectangle representing the laboratory table where the beamline is placed. This rectangle has been discretized with a regular grid. For each point of the grid a score parameter or figure-of-merit is evaluated. This parameter is used to summarize the performances of the beamline at each focal point. It is a number that varies from 0 to 10. The value 10 is assigned when all

requirements are perfectly fulfilled, the value 0 means that at least one of the critical requirement has not been reached. The calculation of the score value goes as follows. First the score value is related to the bandwidth. The score is 10, if the bandwidth is greater than 1000 eV, then 9 if it is between 900 eV and 1000 eV, and so on, until 0 when it is lower than 100 eV. Second, the resolution is checked, if it is greater than 10 eV, then the score is set to zero. Third, if the energy is not in the range 5 - 20 keV, the score is set to zero. Mechanical constraints are taken into account: if the crystal is too bent it will break or a non-elastic deformation can occur. To avoid this situation we calculate the radius of curvature, and if it is smaller than 2.0 m, the score is set to zero. Finally another mechanical constrain is considered, since optical elements are physical objects, they cannot pass through each other. The overlapping can occur when the beamline is build in a narrow environment, and the design of the beamline must consider their extension as well. Therefore whenever two elements overlaps the score is set to zero. An analytical definition of the score parameter is the following:

$$S_{band} = \begin{cases} 0 & \text{if } \Delta_E < 100 \\ 1 & \text{if } \Delta_E \in [100, 200] \\ \dots & \\ 10 & \text{if } \Delta_E > 1000 \end{cases} \quad S_{res} = \begin{cases} 0 & \text{if } \delta_E > 10 \\ 1 & \text{if } \delta_E \leq 10 \end{cases} \quad S_{ene} = \begin{cases} 1 & \text{if } E \in [5, 20] \text{keV} \\ 0 & \text{otherwise} \end{cases} \quad S_{rad} = \begin{cases} 1 & \text{if } R > 2\text{m} \\ 0 & \text{otherwise} \end{cases}$$

where  $\Delta_E$  is the energy bandwidth,  $\delta_E$  the energy resolution,  $E$  the energy and  $R$  the radius of curvature.  $S_{band}$ ,  $S_{res}$ ,  $S_{ene}$ ,  $S_{rad}$  are auxiliary terms that helps to write down the equation for the score parameter  $S$ :

$$S = S_{band}S_{res}S_{ene}S_{rad} \quad (1)$$

We call *figure-of-merit* the plot of the score parameter on the grid. The aim of the simulation is to find a region of the figure of merit which is different from zero and, moreover, to see if part of this region is close to the crystal, so that the beamline is will result compact. Two approaches have been used to define and then optimize the dispersive XAFS beamline. First an analytical approach using simple optical formulas to quantify the energy resolution and bandwidth. This approach is necessary to define the main parameters for the ray-tracing simulation. Each theoretical result has been further verified by ray-tracing simulations. SHADOW3<sup>7</sup> has been used for the ray-tracing, because it tracks the electrical field throughout the optical elements, allowing to compute the intensity at each step.

### 3. ENERGY BANDWIDTH AND ENERGY RESOLUTION

#### 3.1 Analytical results

The definition of energy bandwidth and energy resolution is best seen in the following example. Let consider a simple optical system, which consists of a point size source S, a bend cylindric crystal AB and a camera A'B', as shown in Fig. 3.

The angle  $\widehat{SAA'}$  defines the limiting energy  $E_A$ , while  $\widehat{SBB'}$  defines  $E_B$ , and  $E_A > E_B$ . The energy band is given by  $\Delta E = E_A - E_B$ . If the source has a given size, then one has to consider several close points for the source. In case the source size is very small with respect the size of the mirror, then one can approximate the contribution to the bandwidth of the source, considering the point source solution plus a correction term. The following expression for the **energy bandwidth** is obtained from the derivative of the Bragg's law:

$$\left(\frac{\Delta E}{E}\right)_{band} = \cot \theta_B \sqrt{\omega_D^2 + \left(\frac{p}{R_t \sin \theta_B} - 1\right)^2 \Delta_{src}^2 + \left(\frac{s}{p}\right)^2} \quad (2)$$

where  $\omega_D$  is the Darwin width,  $p = \overline{SC}$ ,  $R_t$  is the radius of curvature of the crystal,  $\Delta_{src} = \widehat{ASB}$  and  $S$  is the source size. The three terms inside the square root are respectively: the Darwin width; a term that depends on the geometry of the crystal and on the source divergence, that becomes zero in the Rowland configuration; and a term that depends on the size of the source. The term **energy resolution** denotes the energy spread seen by

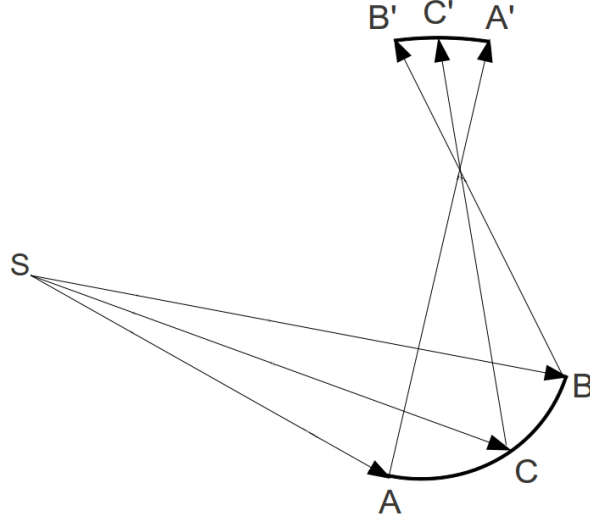


Figure 3. Schematic top view the bent crystal polychromator AB (arbitrary units). S is the source, F is the sample position and A'B' is the detector plane.

the point C'. In an ideal case, i.e. a point-size source and an aberration free optics, it is expected to be a very peaky distribution centered at  $E_c$ . In fact, only the Darwin width contributes to the intensity distribution and the source size is the leading term that controls the energy resolution. To estimate the energy resolution one can apply Eq. 2, considering that only a small portion of the crystal around C reflects the photons that will contribute to C'. Therefore giving an estimation of the energy resolution means estimate the energy bandwidth, but for a very tiny crystal. That is equivalent to reduce the dispersion  $\Delta_{src}$ . In the limit of small angle  $\Delta_{src} \rightarrow 0$  the energy resolution is:

$$\left(\frac{\Delta E}{E}\right)_{res} = \cot \theta_B \sqrt{\omega_D^2 + \left(\frac{s}{p}\right)^2} \quad (3)$$

The analytical *formula* for the bandwidth arises from the fact that  $\Delta E$  comes from three components of  $\Delta \theta$  added in quadrature as stated in subsection.3.1. These three terms are added in quadrature, meaning that each contributions is considered to be gaussian, in a good approximation. The energy resolution is obtained by setting one of the components to zero.

The two *formulae* above are useful tools to estimate the energy band and the resolution. They will be used to compare the results of the numerical simulations, as well.

### 3.2 Ray-tracing results

We used the ray-tracer SHADOW3 to measure the energy bandwidth and the resolution of the optical system. In order to calculate the bandwidth we follow this definition. On the detector, we plot the intensity over the energy band and measure the bandwidth, FWHM. We expect the bandwidth to be of the order of the analytical value  $\Delta E$ . So the rays coming out from the source are set to have an energy distribution between  $E_c - \Delta E$  and  $E_c + \Delta E$ . The expected result instead will range between  $E_c - \Delta E/2$  and  $E_c + \Delta E/2$ . So far, when looking at the plot we will be able to see that the optical system has filtered out some energies. This process has to be repeated for each point of the grid and therefore has been automatized.

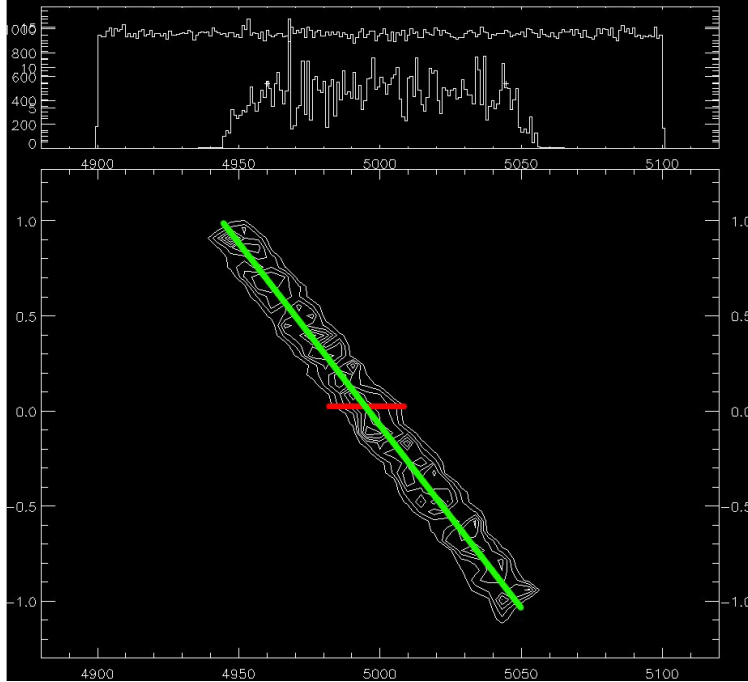


Figure 4. Contour plot weighted with intensity at the detector plane for  $R_t = 2$  m and  $E_c = 5$  keV. Energy in eV along the X axis, positions on the camera in cm.

The resolution calculation is carried out in the following way. The energy of the source rays is now uniformly distributed from  $E_c - 4\delta E$  to  $E_c + 4\delta E$ . This spectrum is large enough to show the linear correlation between the position and the energy, as shown in Fig.4. In this figure the energy of the photons, on the X axis, versus the position reached on the camera, on the Y axis has been plotted. The curves form the map of the intensity distribution on the plane. To give a rough idea of the effect of the source size, if one increases it, then the resulting strip shown in the plot will be thicker. The goal of the method is to find out the thickness at a given position of this strip (or the length of the red segment in Fig. 4). In order to do so, one can find the correlation between the energies and the positions weighted with intensity using a linear regression, which should lead to a line like the green one in Fig. 4.

Another practical parameter related to the energy resolution is the pixels size.

To resolve two energy lines on the camera, two features ought to be satisfied. First the signals must not overlap and second the distance between two peaks on the camera must be greater then the pixel size. To verify that we compared two simulations with a monochromatic source, the first one with the energy fixed by the Bragg angle, the second one with an energy greater then the previous one by  $\delta E$ . We choose a *criterion* that can be easily implemented in a code and it is represented in Fig. 5. If the two segments of FWHM are overlapping then it is not possible to distinguish between the two peaks. This simplification is reasonable because it represents a real experimental situation. In case the peaks are distinguishable we can also measure their distance, and check if it is larger than the pixel size. The pixels of the proposed camera (the FReLoN) - measure  $14 \mu\text{m}$ .

#### 4. SIMULATION OF THE OPTICAL SYSTEM

The simulation work-flow is shown in Fig. 7. For each point of the grid (see Fig. 6) the values of the ray of curvature for the crystal, the energy, the theoretical bandwidth and resolution are calculated. The score parameter described in Sec.2 is then evaluated. If it is different from zero, then the bandwidth and the resolution are recalculated with the ray-tracing methods, otherwise it is rejected.

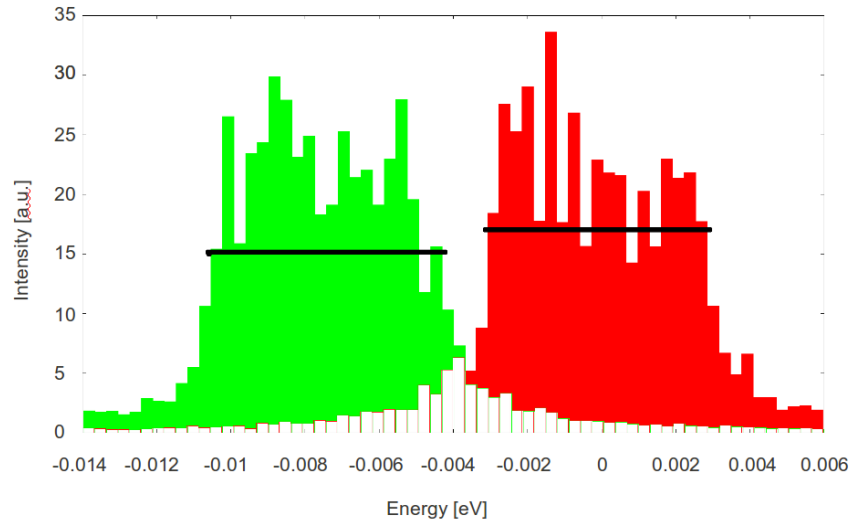


Figure 5. Intensity of two monochromatic beams on the detector. Two histograms overlapped with different colors, the overlapped area is not filled with color. The black line represent the segment obtained with FWHM, in this figure, the two peaks can be distinguished.

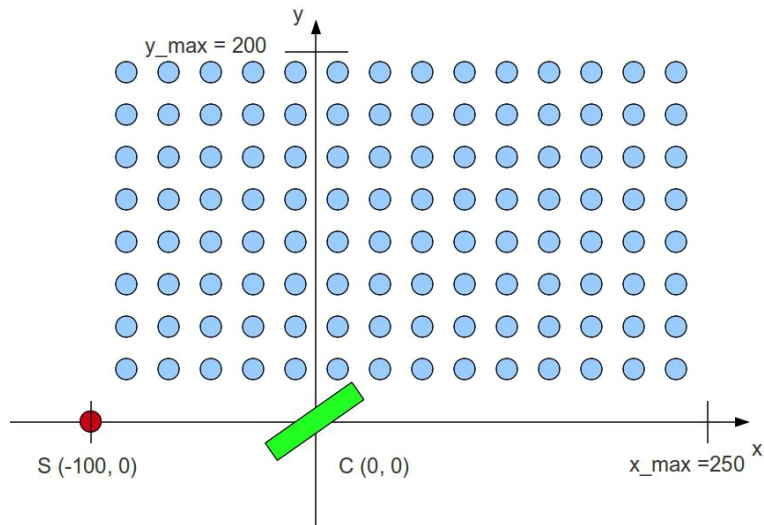


Figure 6. Top view of the grid matching the position of the sample on the table. arbitrary unit.

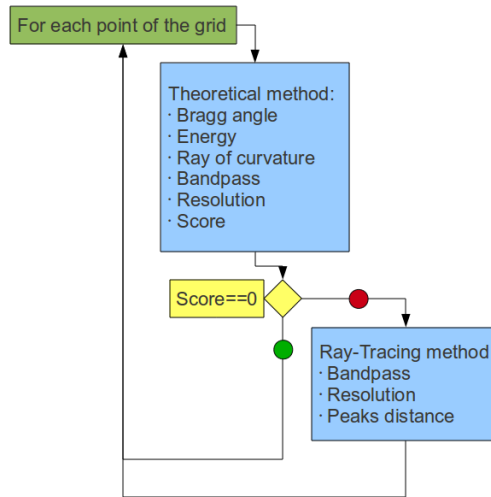


Figure 7. Work-flow of the simulation.

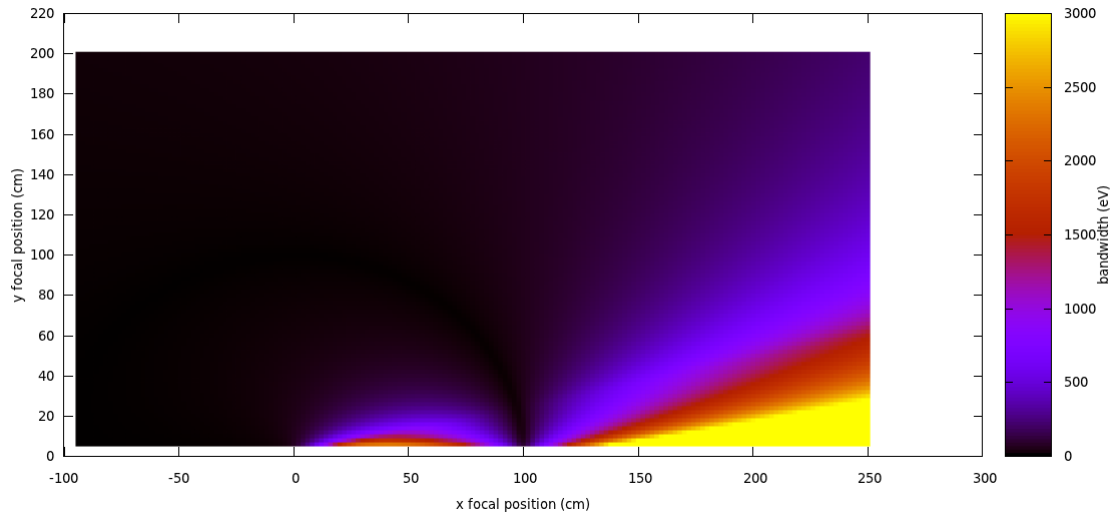


Figure 8. Analytical calculation of the energy bandwidth (eV). Horizontal (X) and vertical (Y) represent the possible sample positions, corresponding to the grid in Fig. 6.

#### 4.1 Results

The analytical energy bandwidth, see Fig. 8, shows two regions of the plane where the score will be high. Synchrotron beamlines are designed to work in the triangular region after the crystal where the bandwidth is very large. Indeed beamlines have no issue of length and they can take advantage of the good properties of this region. Although another region shows good bandwidth as well, the one within a circle, actually only half of it is shown in the figure. The circle is known in optics as the Rowland circle. It is clear that the first region is more suitable for experiments. Nevertheless the last one is very interesting, because it is very close to the crystal and allows for a compact configuration of the beamline. The resolution in energy of the optical system is shown in Fig. 9. The figure shows that the energy resolution is always less than 10 eV in the two regions of interest.

The score parameter (or figure-of-merit) are shown in Fig. 10. It confirms what it was conjectured before about the two regions, the circular and the triangular, where a beamline for XAFS purposes can be designed. In fact all the focal points in the two regions have values different from zero and the score in the triangular region

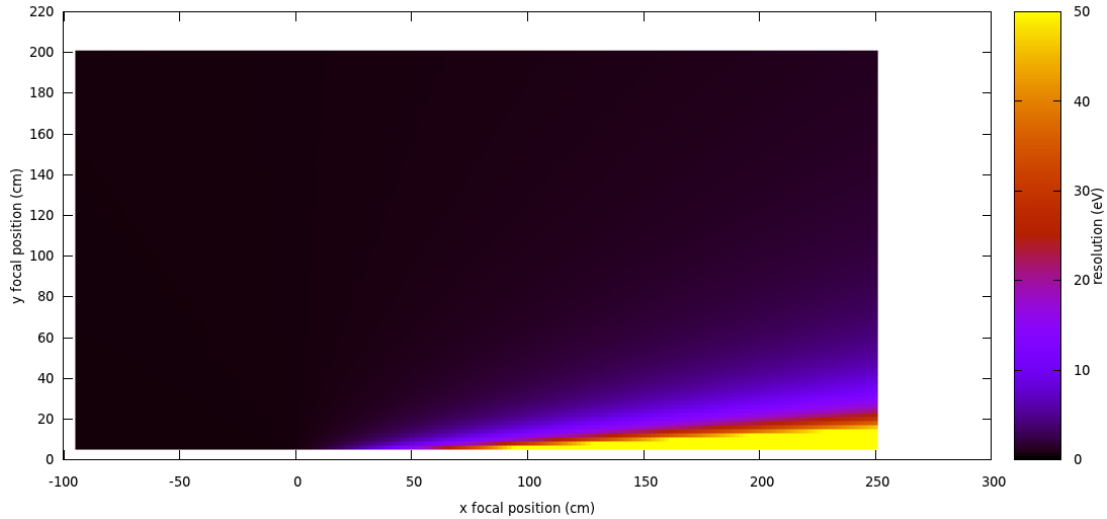


Figure 9. Analytical calculation of the resolution in energy (eV) Horizontal (X) and vertical (Y) represent the possible sample positions, corresponding to the grid in Fig. 6.

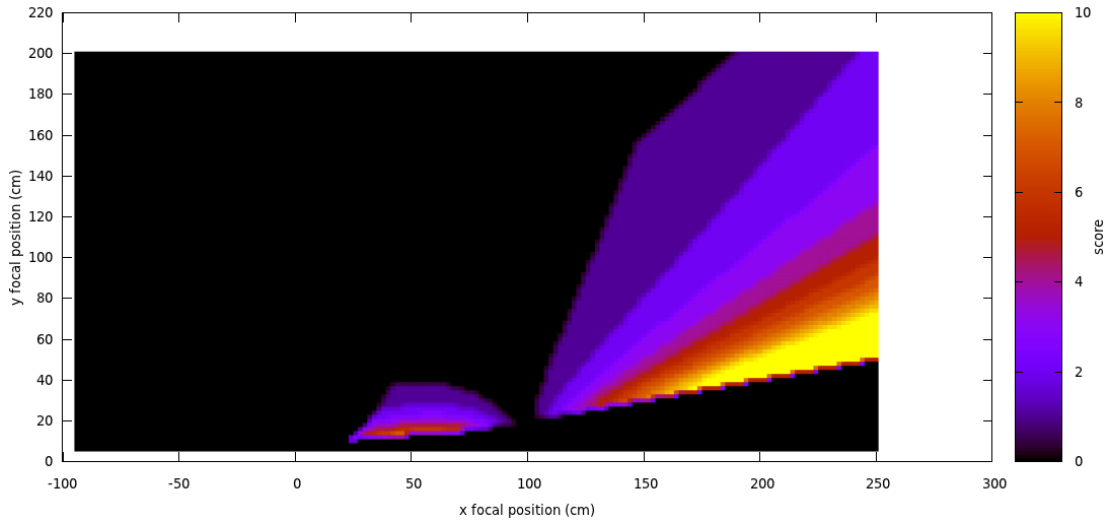


Figure 10. The figure of merit shows where it is possible to perform XAFS analysis. Horizontal (X) and vertical (Y) represent the possible sample positions, corresponding to the grid in Fig. 6.

is generally higher. This figure shows also that mechanical constraints are not an issue in these two regions and they allow for XAFS experiments in the whole range of energy (5 - 20 keV).

When the score differs from zero a ray-tracing simulation is performed. The results for the bandwidth are shown in Fig. 11 and in Fig. 12 the ones for the resolution in energy. These figures must be compared with the previous ones. The comparison is shown in Fig. 13 and Fig. 14 for energy band and energy resolution respectively. The data are compared with the following value, which we call normalized difference:

$$d = \frac{|(\Delta E)_{the} - (\Delta E)_{sim}|}{(\Delta E)_{the}} \quad (4)$$

One obtains that the simulated bandwidths are half of the theoretical ones, on average. And the same for the energy resolution. It is possible to explain this mismatch looking at the theory. The analytical formula arise

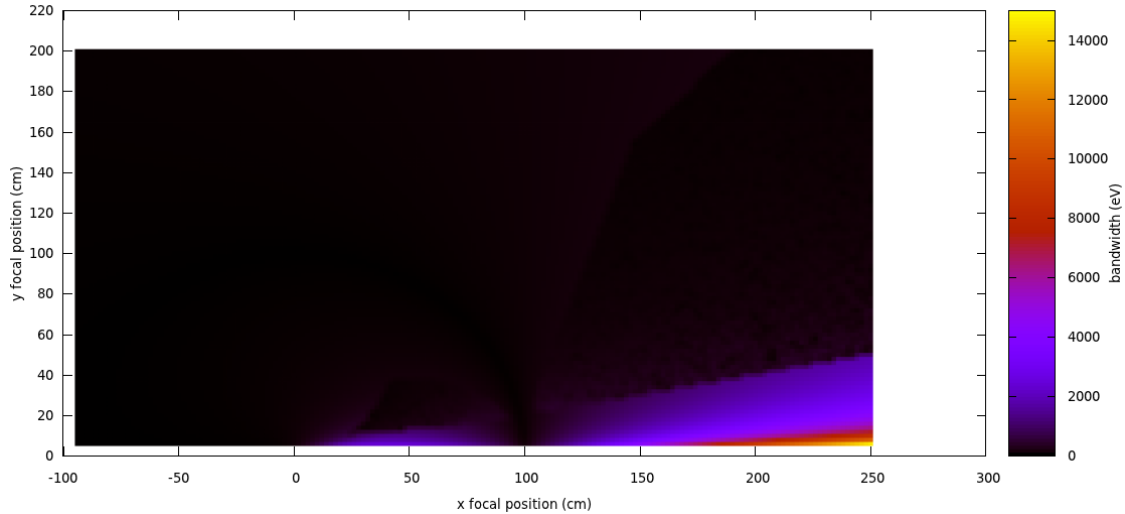


Figure 11. Ray-tracing simulated energy bandwidth (eV). Horizontal (X) and vertical (Y) represent the possible sample positions, corresponding to the grid in Fig. 6.

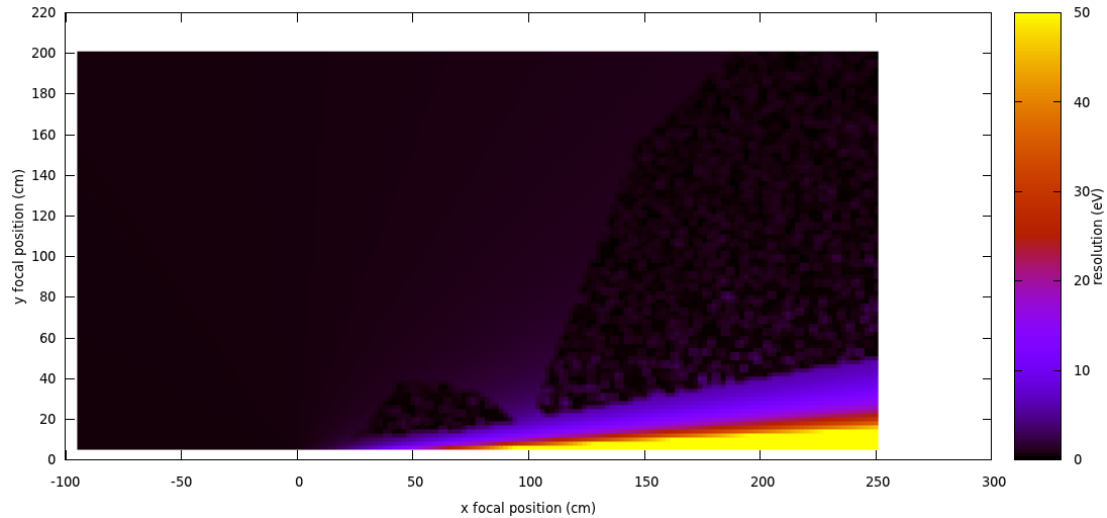


Figure 12. Ray-tracing simulated energy resolution (eV). Horizontal (X) and vertical (Y) represent the possible sample positions, corresponding to the grid in Fig. 6.

from the fact that  $\Delta E$  comes from three components of  $\Delta\theta$  Eq.2. So no one expects a perfect match with the ray-tracing results. The results are nevertheless acceptable, both for bandwidth and for resolution.

The ray-tracing can also evaluate the distribution of intensities over the position on the camera. Two distributions generated with two monochromatic beam of energies  $E_0$  and  $E_1 = E_0 + (\Delta E)_{res}$  are recorded and the distance between the peaks is obtained. We obtain that a pixel size greater than  $50 \mu\text{m}$  is enough to resolve  $\Delta E$  of few eV.

## 5. SUMMARY AND CONCLUSIONS

A conceptual design of a dispersive XAFS beamline using the X-ray source MIRRORCLE has been presented. The relevant quality parameters for the optics have been calculated and a figure of merit summarizes the results. These calculations are used to meet the experimental requirements in terms of energy bandwidth and resolution

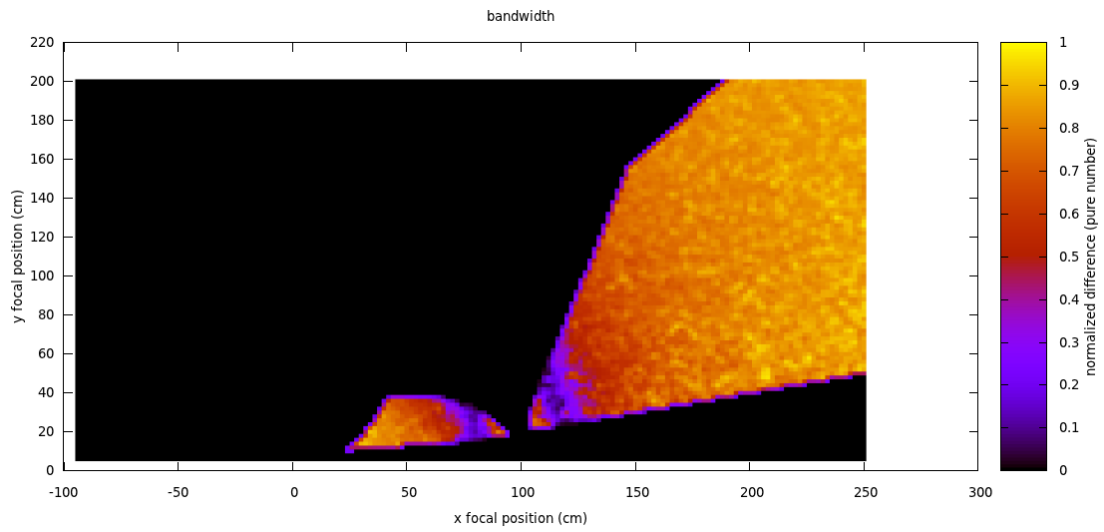


Figure 13. Evaluation of bandwidth difference between theory and simulation. Horizontal (X) and vertical (Y) represent the possible sample positions, corresponding to the grid in Fig. 6.

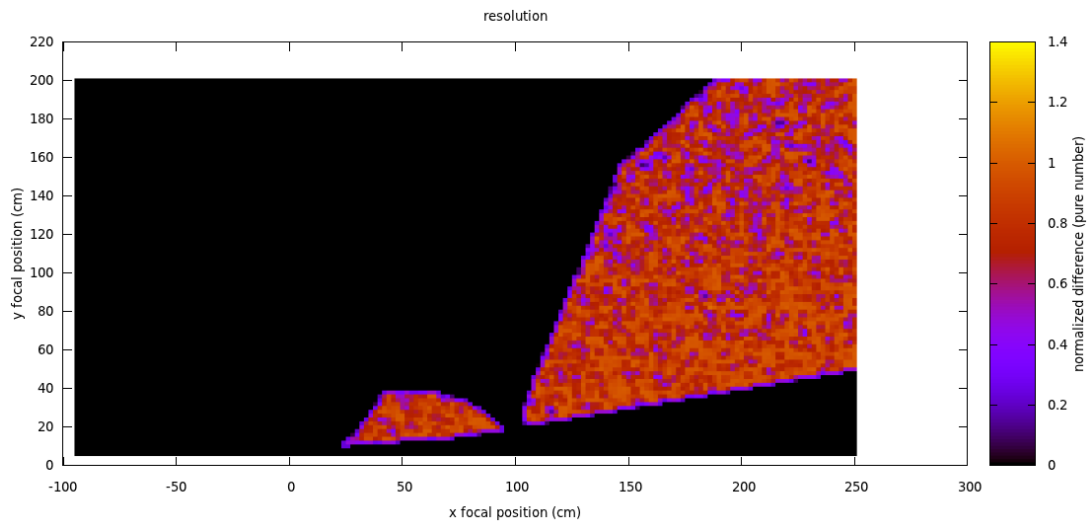


Figure 14. Evaluation of resolution difference between theory and simulation (pure number). Horizontal (X) and vertical (Y) represent the possible sample positions, corresponding to the grid in Fig. 6.

that finally comes to place the sample at appropriate positions. It is shown that by placing the sample inside the Rowland circle, a more compact beamline can be obtained, even though the score parameter is higher in the region outside the Rowland circle. The next important quantity to study is the flux. We have used X-ray tracing to evaluate the beamline transmittance. The number of photons at the sample and at each detector pixel is calculated by scaling the beamline transmittance with the source spectrum. The minimum flux (photons/s/mrad/eV bandwidth) necessary to obtain a given number of counts at each detector's pixel can be thus obtained.

## 6. ACKNOWLEDGEMENTS

This project has been funded by the European Union FP7 Infrastructures LABSYNC (grant number 213126).

## REFERENCES

- [1] [http://www.photonproduction.co.jp/en/index\\_e.htm](http://www.photonproduction.co.jp/en/index_e.htm).
- [2] Yamada, H., "Novel X-ray Source Based on a Tabletop Synchrotron and Its Unique Features," *Nuclear Instruments and Methods in Physics Research B* **199**, 509–516 (2003).
- [3] Marziani, M., Taibi, A., Di Domenico, G., and Gambaccini, M., "Optimization of radiography applications using X-ray beams emitted by compact accelerators. Part I: Monte Carlo study of the hard x-ray spectrum," *Medical Physics* **36**, 4683–4701 (2009).
- [4] [http://www.photonproduction.co.jp/en/application\\_e/medical\\_e.htm](http://www.photonproduction.co.jp/en/application_e/medical_e.htm).
- [5] [http://www.photonproduction.co.jp/en/application\\_e/nondestructive\\_e.htm](http://www.photonproduction.co.jp/en/application_e/nondestructive_e.htm).
- [6] [http://www.photonproduction.co.jp/en/application\\_e/XAFS\\_e.htm](http://www.photonproduction.co.jp/en/application_e/XAFS_e.htm).
- [7] Sanchez del Rio, M., Canestrari, N., Jiang, F., and Cerrina, F., "SHADOW3: a new version of the synchrotron X-ray optics modelling package," *Journal of Synchrotron Radiation* **18**, 708–716 (2011).